

Characterization and Low-Resolution Structure of an Extremely Thermostable Esterase of Potential Biotechnological Interest from *Pyrococcus furiosus*

F. Mandelli¹ · T. A. Gonçalves^{1,2} · C. A. Gandin³ · A. C. P. Oliveira^{1,2} · M. Oliveira Neto³ · F. M. Squina¹

Published online: 24 September 2016
© Springer Science+Business Media New York 2016

Abstract Enzymes isolated from extremophiles often exhibit superior performance and potential industrial applications. There are several advantages performing biocatalysis at elevated temperatures, including enhanced reaction rates, increased substrate solubility and decreased risks of contamination. Furthermore, thermophilic enzymes usually exhibit high resistance against many organic solvents and detergents, and are also more resistant to proteolytic attack. In this study, we subcloned and characterized an esterase from the hyperthermophilic archaeon *Pyrococcus furiosus* (Pf_Est) that exhibits optimal activity around 80 °C using naphthol-derived substrates and *p*-nitrophenyl palmitate (*p*NPP). According to the circular dichroism spectra, the secondary structure of *P. furiosus* esterase, which is predominantly formed by a β -sheet structure, is very stable, even after incubation at 120°C. We performed SAXS to determine the low-resolution structure of Pf_Est, which is monomeric in solution at 80 °C and has a molecular weight of 28 kDa. The K_m and V_{max} values for

this esterase acting on *p*NPP were 0.53 mmol/L and 6.5×10^{-3} U, respectively. Pf_Est was most active in the immiscible solvents and retained more than 50 % in miscible solvents. Moreover, Pf_Est possesses transesterification capacity, presenting better results when isobutanol was used as an acyl acceptor ($2.69 \pm 0.14 \times 10^{-2}$ $\mu\text{mol}/\text{min mg}$) and the highest hydrolytic activity toward olive oil among different types of oils testes in this study. Collectively, these biophysical and catalytic properties are of interest for several biotechnological applications that require harsh conditions, including high temperature and the presence of organic solvents.

Keywords Hyperthermophilic · kinetics parameters · Transesterification · Circular dichroism · SAXS

Introduction

Lipases and esterases are lipolytic enzymes that make up an important group of enzymes which play a role in the metabolism of lipid degradation. Most of the lipases used in industry are of fungal and bacterial origin [1, 2].

Lipolytic enzymes are very attractive for industrial applications such as the detergent, oleochemical, pulp and paper industries, synthesis of flavor esters, and resolution of chiral drugs [3–6].

These enzymes can be used as catalysts to cleave ester bonds in aqueous media and in organic media, which can catalyze formation of ester bonds via esterification, inter-esterification, and transesterification reactions [7]. It was also stated that esterases degrade natural materials and industrial pollutants such as cereal wastes, plastics, and other toxic chemicals [8].

Electronic supplementary material The online version of this article (doi:10.1007/s12033-016-9975-5) contains supplementary material, which is available to authorized users.

✉ F. M. Squina
fabio.squina@bioetanol.org.br

¹ Laboratório Nacional de Ciência e Tecnologia do Bioetanol (CTBE), Centro Nacional de Pesquisa em Energia e Materiais (CNPEM), Rua Giuseppe Máximo Solfaro, n° 10000, Campinas, SP 13083-970, Brazil

² Departamento de Bioquímica, Instituto de Biologia (IB), Universidade Estadual de Campinas (UNICAMP), Campinas, SP, Brazil

³ Departamento de Física e Biofísica, Instituto de Biociências de Botucatu, UNESP Univ Estadual Paulista, Botucatu, SP, Brazil

Thermophilic enzymes are known due to their higher stability against the denaturing action of heat and chemical denaturants when comparing to mesophilic enzymes. As a result, they can be used as biocatalysts under rather harsh environmental conditions [9].

The hyperthermophilic archaea *Pyrococcus furiosus* was first isolated by Fiala and Stetter [10] from a Vulcano Island near southern Italy. This hyperthermophilic archaeon is an obligate anaerobic heterotroph that grows optimally at 100 °C. *P. furiosus* is also a source of several industrially important enzymes [11].

In this study, we report gene subcloning and expression, followed by purification, functional and biophysical characterization, along with low-resolution structure of an esterase from *Pyrococcus furiosus* (Pf_Est). Thus, the biochemical and biophysical characterization of Pf_Est reveals its potential to be used in biotechnological applications.

Materials and Methods

Synthesis of the Esterase Coding Sequence

In this study, we show a characterization of a hyperthermophilic esterase from *Pyrococcus furiosus*. The region of the gene AFN03900.1 (amino acids 160–404), predicted as an esterase was synthesized (GenOne Biotechnologies—Rio de Janeiro, Brazil) by a solid-phase synthesis using phosphoramidite method [12] (Figure S1). The gene was synthesized based on the nucleotide sequence, delivered in the vector pBluescript II SK (Figure S2), and digested with the *Nhe*I and *Bam*HI restriction enzymes and then inserted into the expression vector pET-28a. Sanger sequencing (3500×L Genetic Analyzer, Thermo Scientific) was performed to check the sequence accuracy of the subcloned DNA fragment. The pET28a/Pf_Est plasmid was transformed in expression cell, as explained below.

Protein Expression and Purification

Escherichia coli BL21 (DE3) was transformed with the pET28a/Pf_Est plasmid and plated in selective solid LB medium containing kanamycin (50 µg/mg). Cells from a single colony were grown in 8 mL of liquid LB-kanamycin (at the same previous concentration) for 16 h at 37 °C and 250 rpm. After that, this culture was passed to 800 mL of fresh LB-kanamycin medium and grown under the same conditions until reaching an optical density of 0.6 at 600 nm. Afterward, the recombinant protein expression was induced by adding 0.5 mmol/L IPTG. After 4 h, the cells were harvested at 8500 g and stored at –20 °C. The cells were again suspended using lysis buffer (20 mmol/L

sodium phosphate pH 7.5, 100 mmol/L NaCl, 5 mmol/L imidazole, 80 µg/mL egg lysozyme, and 5 mmol/L PMSF), followed by mechanical cell disruption (Ultrasonic Processor, Sonics Vibracell). Finally, the extract was centrifuged at 10,000g for 30 min at 4 °C.

The Pf_Est was purified by chromatography using an ÄKTA FPLC system (GE Healthcare). The cell supernatant was loaded onto a 5 mL HiTrap Chelating HP column (GE Healthcare) charged with Ni²⁺ and pre-equilibrated with 20 mmol/L sodium phosphate pH 7.5, 100 mmol/L NaCl, 5 mmol/L imidazole (buffer A) at 1 mL/min. The column was washed with 10 column volumes (CVs) of buffer A to remove unbound fractions, and the enzyme fractions were eluted using a nonlinear, imidazole gradient from 5 to 500 mmol/L (buffer B—20 mmol/L sodium phosphate pH 7.5, 100 mmol/L NaCl, and 500 mmol/L imidazole) in 20 CVs. The protein fractions were pooled and concentrated to 2 mL using a 10 kDa-pore Amicon, then a second purification step was performed using a Superdex 200 10/300 GL column (GE Healthcare), which was pre-equilibrated and eluted with 20 mmol/L sodium phosphate buffer pH 7.5 containing 100 mmol/L NaCl at flow of 0.5 mL/min; elution was monitored at 280 nm. Enzyme purification was analyzed by sodium dodecyl sulfate polyacrylamide gel (SDS-PAGE).

Enzyme Activity Assays

The esterase activity was assessed using the substrates α -naphthyl acetate and α -naphthyl butyrate according to the methods previously described [13]. Briefly, the enzymatic solution (20 µL at 0.5 mg/mL) was mixed with 20 µL of sodium acetate buffer (100 mmol/L, pH 5.5) and 10 µL of substrate (50 mmol/L). The reaction was incubated at 80°C for 30 min, then 50 µL of fast garnet salt (0.1 % w/v and SDS 15 % w/v in DMSO) was added and the absorbance was read at 560 nm. Pf_Est was also assayed using *p*-nitrophenyl palmitate (*p*NPP, Sigma-Aldrich) as the substrate. The reaction was conducted by mixing 30 µL of *p*NPP (10 mmol/L in isopropanol), 110 µL of the buffer (Tris HCl pH 8.0 + Arabic Gum 0.1 % w/v + Triton X100 0.4 % w/v), and 10 µL (0.5 mg/mL) of the purified enzyme. The reaction was incubated at 80°C for 20 min, and then the absorbance was read at 410 nm [14]. A control reaction was measured with the absence of the enzyme for both assays. The standard curves using 10 different concentrations of 1-Naphthol (Sigma-Aldrich) and 4-nitrophenol (Sigma-Aldrich) were used for the enzyme quantification assays. The equation obtained for adjustment of the 1-Naphthol curve was $y = 71.922x + 0.0123$ with $R^2 = 0.9966$ and for 4-nitrophenol was $y = 61.41x$ with $R^2 = 0.9946$. One unit of esterase activity was defined as the amount of enzyme required to release 1 µmol of

product (4-nitrophenol (pNP) when the substrate utilized was the pNPP and 1-naphthol when the substrates utilized were α -naphthyl acetate and α -naphthyl butyrate) per minute. To obtain the specific activity, this value was divided by the amount of protein utilized in each assay. All assays were performed in triplicate. The specific activities of purified enzyme for each purification step were evaluated.

Determination of Optimum pH, Temperature, and Kinetic Parameters

The optimum pH and pH stability were determined by measuring the enzymatic activity in different buffers at 100 mmol/L (glycine–HCl pH 2.6, citrate buffer pH 3.6–6.0, phosphate buffer pH 6.5–8.0, and glycine NaOH buffer pH 9.0–10.4). The optimum pH was estimated at 80 °C using three substrates: α -naphthyl acetate, α -naphthyl butyrate, and pNPP. The pH stability was estimated by the incubation of Pf_Est for 30 min in the different pHs followed by the evaluation of the remaining activity by pNPP assay.

The optimum temperature was estimated by measuring the relative enzyme activity, using α -naphthyl acetate, α -naphthyl butyrate, and pNPP as substrates, at various temperatures (55–100 °C) using 100 mmol/L sodium acetate buffer at pH 5.5 (for assays with α -naphthyl substrates) and 50 mmol/L Tris–HCl pH 8.0 (for assays with pNPP). The temperature stability was performed by incubation of Pf_Est at 65, 75, 85, and 120 °C until enzymes loses more than 50 % of its activity. Afterward, the enzymatic activity was evaluated using pNPP as substrates.

The stability analysis of Pf_Est in solvents was performed according to Sande et al. [15]. Briefly, the pure enzyme was incubated with two concentrations (5 and 50 % v/v—solvent/Buffer Tris HCl pH 8.0 + Arabic Gum 0.1 % w/v + TritonX 100 0.4 % w/v) of water-miscible solvents (methanol, ethanol, 2-propanol, and isobutanol) and water-immiscible solvents (*n*-hexane and dichloromethane) at 60 °C for 30 min and then the enzymatic activity was dosed using pNPP.

Kinetic parameters were determined against pNPP, where the substrate concentrations ranged from 0.05 to 6.0 mmol/L. K_m , V_{max} , and k_{cat} values were calculated using GraphPad Prisma 6.0 (GraphPad Software), based on the Michaelis–Menten enzyme kinetic model.

Circular Dichroism Spectroscopy and Thermal Denaturation

Circular dichroism spectroscopy and thermal denaturation were performed according to Mandelli et al. [16]. The far-UV CD spectra were recorded, from 190 to 260 nm, in a

1-mm quartz cuvette using a spectropolarimeter (Jasco J-810—Jasco International Co. Ltd., Japan), equipped with a Peltier temperature control unit. The purified enzyme (0.2 mg/mL) diluted in 75 mmol/L of sodium phosphate buffer, pH 7.5, was used for collection of spectral data. For thermal scans, the protein samples (0.2 mg/mL) were heated from 20 to 100 °C and subsequently cooled to 20 °C with a heating/cooling rate of 1 °C/min, controlled by a Jasco programmable Peltier element. Moreover, the enzyme was heated at 120 °C for 15 min in an incubator (TE 393/2—Tecnal, Brazil) and then the far-UV CD spectra were recorded.

Small Angle X-ray Scattering

Small angle X-ray scattering (SAXS) data were collected at the SAXS2 beamline at the Brazilian Synchrotron Light Laboratory (LNLS). The wavelength of the incident radiation was set to $\lambda = 1.55 \text{ \AA}$ and the X-ray patterns were recorded with a two-dimensional CCD detector. The sample detector distance was 1040.48 mm, resulting in a scattering vector range of $0.016 < q < 0.313 \text{ \AA}^{-1}$, where q is the magnitude of the q-vector defined by $q = 4\pi \sin(\theta)/\lambda$ (2θ is the scattering angle). Data were collected at 80 °C, which corresponds to the optimum temperature of the enzyme and in concentrations of 0.5, 1, and 5 mg/mL in 20 mmol/L phosphate buffer, 100 mmol/L NaCl, and pH 7.5. The SAXS patterns were corrected for the detector response and scaled by the incident beam intensity and absorption of the samples. The background scattering curve was subtracted from the corresponding sample scattering. Integration of the SAXS patterns was performed using the Fit2D software [17]. SAXS data were analyzed according to Alvarez et al. [18]. Briefly, the programs used in SAXS analyses were GNOM software [19], SAXSmow [20], GASBOR [21], CRY SOL [22], and SUPCOMB [21].

Transesterification and Hydrolytic Activity

The transesterification activity was measured according to Shih and Pan [14] with some modifications. Briefly, 0.25 mg of the lyophilized enzyme was mixed in 10 mmol/L of pNPP and 1 mol/L of alcohol (ethanol, methanol, isopropanol, and isobutanol), and the final volume was adjusted to 1 mL with hexane. The reaction was incubated for 1 h at 60 °C and 800 rpm, and then 1 mL of NaOH (0.1 mol/L) was added to the reaction and the liberated pNP was measured in a spectrophotometer at 410 nm. The transesterification activity was defined as the amount of protein required to liberate 1 μmol of pNP per minute under these condition.

To evaluate the hydrolytic capacity of Pf_Est, titrations tests were carried out using different oils (olive, corn, soy, and waste cooking oil) as substrates. The assay was conducted according to Rabbani et al. [23] and Wang et al. [24] with some modifications. The enzymatic reactions, prepared in 50 mL Erlenmeyer flasks, were incubated on a reciprocal shaker at 100 rpm, at 80 °C for 30 min. Each reaction contained 2.0 mL of oil in 11 mL of buffer (100 mmol/L Tris HCl pH 8 + Arabic Gum 0.1 % w/v + Triton X100 0.4 % w/v) and 1 mL of purified enzyme (0.94 mg/mL). A blank reaction was performed without the enzyme. Reaction was stopped by adding 5 mL of ethanol. After the reaction, the released fatty acids were determined by titration with NaOH 0.25 mol/L using bromothymol blue (0.04 %) as a pH indicator. One unit of enzyme activity was defined as 1.0 μ mol of fatty acid liberated per min.

Results

Synthesis of Pf_Est

In this study, we show a characterization of a hyperthermophilic esterase from *Pyrococcus furiosus* (Pf_Est). Pf_Est was synthesized based on the sequence deposited on NCBI (GenBank: AFN03900.1). Although this sequence was annotated as alpha-dextrin endo-1, 6-alpha-glucosidase, the BLAST and Pfam analysis of the region comprehending the amino acids 160–404, result on a CDD and a HMM, of an abhydrolase and esterase, respectively. α/β -hydrolase fold protein class contains esterases, acetylcholinesterases, cutinases, carboxylesterases, and epoxide hydrolases [25]. Moreover, the sequence of the synthesized gene was submitted to I-Tasser analysis, and through the alignment of Pf_Est with other esterases, it was possible to found its catalytic triad (S126, E 181, and H 220), and also the consensus motif Gly-X-Ser-X-Gly, which catalytic serine is embedded (Figure S3). Besides, the biochemical and biophysical characterization of Pf_Est, showed on this manuscript reinforces the esterase activity of Pf_Est.

Biochemical and Biophysical Characterization of Pf_Est

The recombinant Pf_Est enzyme was expressed in the soluble fraction of *E. coli* BL21 (DE3) cells at 37 °C. The enzyme was purified using two chromatographic steps (Fig. 1a, b); and the purified enzyme presented a single band near 28 kDa (Fig. 1c) in the SDS-PAGE analysis as expected. Moreover, the specific activities of purified enzyme for each purification steps are shown in Table 1.

As shown in Fig. 2a, Pf_Est presented activity over a broad pH range with maximum activity at pH 7.0 with α -naphthyl acetate, at pH 6.5 with α -naphthyl butyrate and at pH 8.0 with *p*NPP. Pf_Est was able to retain more than 50 % of its activity from pH 5.5 to 10 with α -naphthyl acetate and from pH 6.5 to 8 with α -naphthyl butyrate. The enzyme stability (Fig. 2c) showed that Pf_Est retain almost 100 % of its activity at pH 7.5 and 8.0 and more than 50 % at pH 6.0–7.0.

For both α -naphthyl substrates, the maximum activity was observed at 80 °C, while for *p*NPP the maximum activity was 5 °C degrees lower (Fig. 2b). Furthermore, the effect of temperature on activity of Pf_Est was examined by monitoring using α -naphthyl acetate, α -naphthyl butyrate, and *p*NPP in the range from 55 to 100 °C. The enzyme was able to retain about 50 % of its activity at 50 and 85 °C for all substrates tested. Pf_Est was heat-stable in all tested temperatures; after 48 h of incubation at 65, 75, 85, and 120 °C, the enzyme conserved 81, 80, 72, and 42 % of the initial activity, respectively (Fig. 2d).

Enzyme stability was tested in different water-miscible and -immiscible solvents in the proportions 5 and 50 %, v/v (solvent/buffer). Pf_Est exhibited tolerance to low concentrations (5 % v/v) of all solvents (Table 2). At higher concentrations, the enzyme was most active in the immiscible solvents and retained more than 50 % of its activity in 2-propanol, isobutanol, and ethanol (Table 2).

The esterase kinetic parameters were calculated from the initial velocities using 12 *p*NPP concentrations ranging from 0.05 to 6.0 mmol/L. Pf_Est obeys the Michaelis–Menten curve as expected [26], where the kinetics parameters were determined from the Michaelis–Menten adjustment of the curve shown in Fig. 2d. The Pf_Est presented a k_{cat} of $1.6 \times 10^{-2} \text{ s}^{-1}$, K_m of 0.53 mM, and V_{max} of $6.5 \times 10^{-3} \text{ U}$, good indicators of an enzyme with great potential for use in biotechnological applications [27].

Jpre4 is a secondary protein structure prediction server, which provides predictions by the JNet algorithm with 82 % accuracy. When submitting the Pf_Est sequence in the server (<http://www.compbio.dundee.ac.uk/jpred/>), a prediction of a protein was generated containing eight beta-sheets and seven alpha-helices.

Change in the secondary structure of Pf_Est was investigated by CD spectroscopy over the temperature range of 20–100 °C (Fig. 2f). A positive band at 195–200 nm and a negative band at 210–220 nm were observed in the far-UV CD spectra, which is a typical profile observed for proteins rich in β -sheet structures [28, 29]. According to the CD spectral data, Pf_Est maintains the secondary structure after incubation at 100 °C. Moreover, the enzyme was also able to preserve its structure after incubation at 120 °C for 15 min (Fig. 2f).

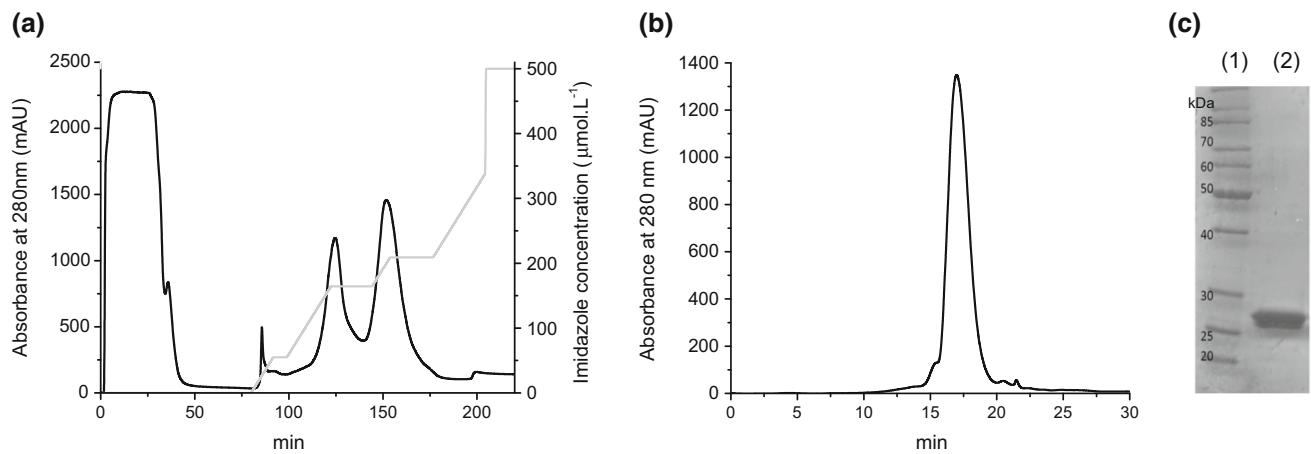


Fig. 1 **a** Elution profile of esterase in the 5 mL HiTrap Chelating HP column. Bound fractions were eluted using a nonlinear imidazole gradient (gray line) ranging from 5 to 500 mmol/L at 1 mL/min. **b** Size-exclusion chromatogram of esterase in a Superdex 200 10/300

column in 20 mmol/L sodium phosphate buffer pH 7.5 containing 100 mmol/L NaCl at 0.5 mL/min. **c** SDS-PAGE analysis of esterase samples: **1** molecular weight marker (Thermo Scientific, USA), **2** purified esterase

Table 1 Specific activities of purified enzyme after each purification step

Steps	Protein (mg)	Activity (U) ^a	Total activity (U/mL) ^a	Specific activity (U/mg) ^a	Fold purification	% Yield
Lysate	205.96	0.060 ± 0.012	11.967 ± 2.447	0.872 ± 0.232	1	100
Ni ²⁺ affinity	12.02	0.024 ± 0.002	4.806 ± 0.368	4.743 ± 0.157	5.44	40
Gel filtration	10.22	0.019 ± 0.001	3.747 ± 0.094	5.654 ± 0.568	6.48	31

^a The activity was calculated using pNPP assay

Molecular Shape Envelope at Low Resolution and Structural Parameters

To evaluate the overall shape and oligomeric state of Pf_Est, SAXS was performed at the optimum temperature and data were collected at three different protein concentrations: 0.5, 1, and 5 mg/mL. The radius of gyration (R_g), obtained by Guinier approximations, presented similar values indicating the absence of interparticle correlation. Thus, further SAXS analysis was performed using data at the concentration of 5 mg/mL.

A Porod constant of 1.10^{-3} was subtracted from the scattering pattern prior to the $p(r)$ analysis due to the high entropy of the system at 80 °C. SAXS curve adjustments in reciprocal and real space were performed using the GNOM package [19] (Fig. 3a, b). The Guinier approximation (Fig. 3a—inset) respected the $q.R_g < 1.3$ limit [30], and the value 21.4 Å is in good agreement with the radius of gyration (R_g) obtained from the $p(r)$, 19.72 Å [19]. The crystallography model of the feruloyl esterase domain of the cellulosomal xylanase z from *Clostridium thermocellum* [31] (PDB id: 1JJF) presents a sequential identity of 27 % compared to Pf_Est, where alignment was performed using blast pdb from the NCBI. The simulated SAXS curve

and comparison with experimental data were conducted with the Crysol package [22] (Fig. 3a). The high-resolution data fit to the experimental data presented a χ^2 value of 5.23. Molecular weight evaluation using SAXSmoW indicated that Pf_Est at 80 °C is present as a monomer in solution, with a discrepancy of 7.5 % from the theoretical value (28.55 kDa) which is expected due to the confidence interval of the method [20]. Dummy residues generated using the real space model correlate well with the crystallographic model (Fig. 3c). Good agreement is shown by the $p(r)$ comparison (Fig. 3b). SAXS-derived parameters are shown in Table 3.

Potential Biotechnological Application of Pf_Est

The esterases are of industrial interest, since they have the capacity to catalyze hydrolytic as well as synthetic reactions. To promote synthetic catalysis, reactions are performed in the absence of water, instead of organic solvents or more recently, ionic liquids [32].

The transesterification activity of Pf_Est was investigated in the presence of four alcohols (methanol, ethanol, 2-propanol, and isobutanol) and *n*-hexane, using pNPP as a

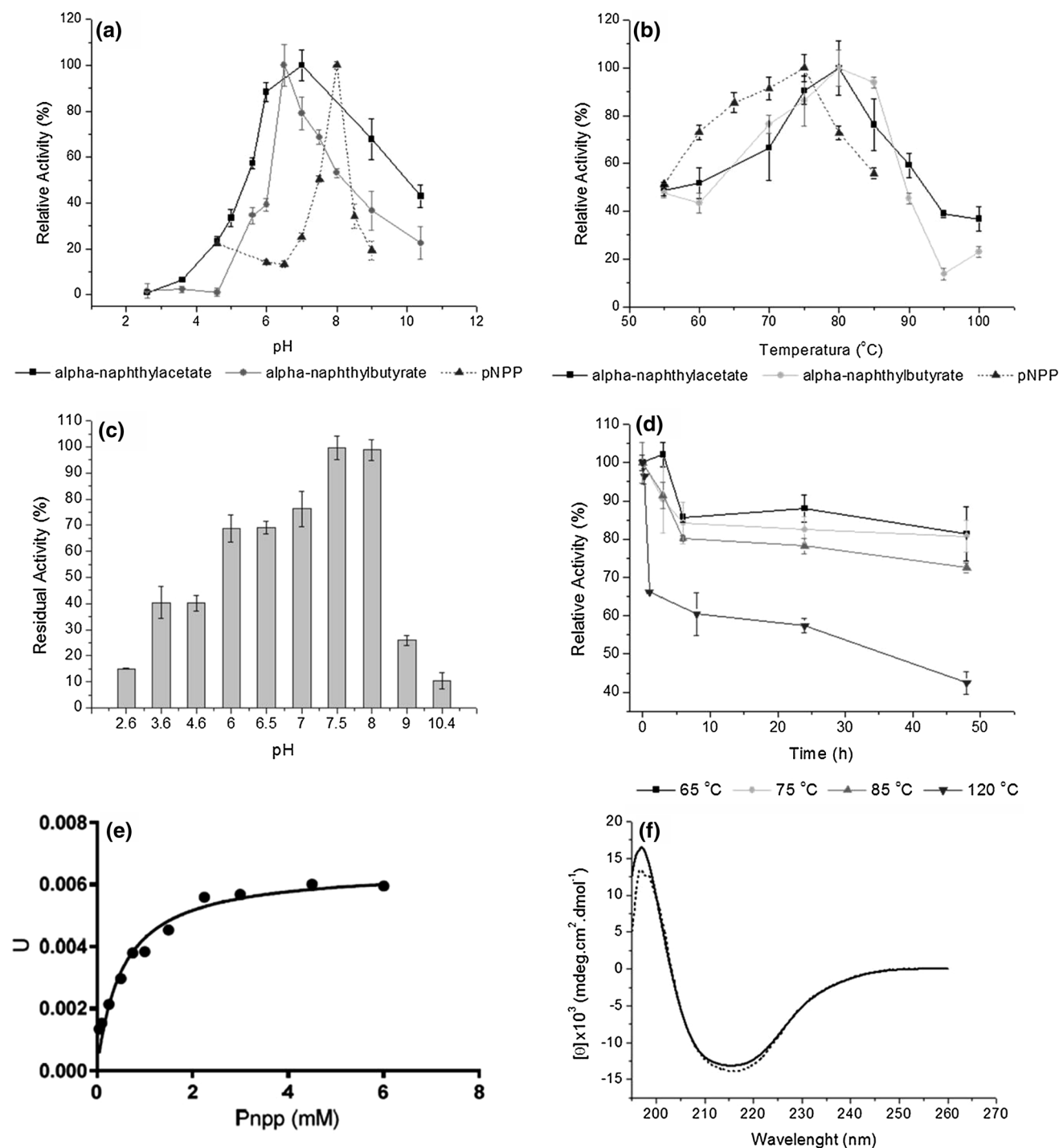


Fig. 2 Optimum pH (a) and temperature (b) and residual pH (c) and temperature (d) of esterase from *P. furiosus*. Michaelis–Menten adjustment made using the software Graph Pad Prism 6.0 (GraphPad Software) to calculate the kinetic parameters of *P. furiosus* esterase, where pNPP was the substrate (e); Far-UV circular dichroism (CD)

spectra of *P. furiosus* esterase. The experiment was carried out with 0.2 mg/mL of esterase in sodium phosphate buffer pH 7.5 at 20 °C. The solid line is the CD spectra of the enzyme at 20 °C and the dashed line is the CD spectra after heating the enzyme to 120 °C for 15 min (f)

substrate (Table 4). The best results were obtained in the transesterification activity with isobutanol while when methanol was used the Pf_Est presented the lowest transesterification activity.

The hydrolytic activity of Pf_Est was tested against several oils and the highest activity was found toward olive oil (6.2 U/mg) followed by soy oil (2.4 U/mg), waste cooking oil (1.8 U/mg), and corn oil (0.9 U/mg).

Discussion

Esterases often show broad substrate spectrum and are widely used as biocatalysts for the synthesis of important materials in pharmaceutical and chemical industries [33].

Table 2 Effects of water-miscible and -immiscible solvents on Pf_Est

Solvents	Residual activity %	
	5 % (v/v)	50 % (v/v)
Isopropanol	90.7	52.7
Isobutanol	118.3	63.9
Methanol	115.2	39.5
Ethanol	102.8	51.5
Hexanol	99.8	111.2
Dichloromethane	213.0	369.0

In this study, the gene encoding a hyperthermophilic esterase from *Pyrococcus furiosus* was synthesized, sub-cloned in an expression vector, expressed in a mesophilic host, purified, and biochemically and biophysically characterized.

Pf_Est presented optimum pH activity at 6.5–7.0 in naphthol-derivate substrates, which is slightly lower than the optimum pH (7.5) reported earlier for esterases from *Brevibacterium linens* ATCC 9174, *Thermus thermophilus* HB27, and *Geobacillus* sp. TF17 [34–36]. The optimum temperature for Pf_Est activity was 80 °C in α -naphthyl acetate (and butyrate) and 75 °C in *p*NPP. Moreover, the half-life of this enzyme at 120 °C is approximately 34 h using *p*NPP as substrate. Previous studies show the Pf_Est half-life of 34 h at 100 °C, 6 h at 110 °C, 2 h at 120 °C, and 50 min at 126 °C [11]. The stability present by Pf_Est is higher than the stability of others enzymes from *P. furiosus* previously described in the literature [37, 38].

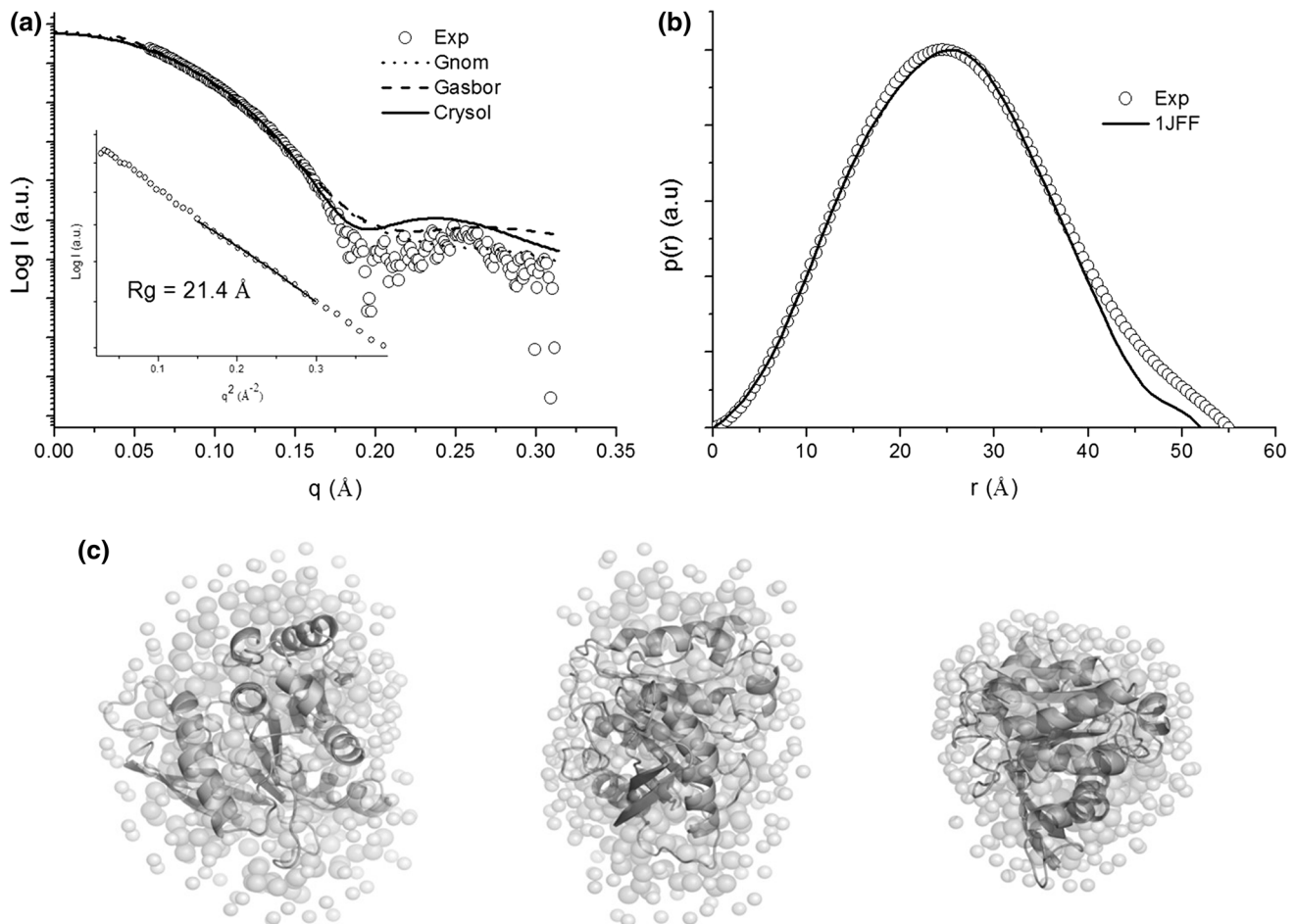


Fig. 3 Experimental SAXS curve of the hyperthermophilic esterase from *P. furiosus* and fitting procedures. *Inset* Guinier's approximation (a). *p(r)* comparison of the experimental data and the crystallographic simulated scattering (b), Superposition of the crystallographic model for the feruloyl esterase domain of the cellulosomal xylanase z of

Clostridium thermocellum [31] (PDB id: 1JFF) with the low-resolution model generated by Gasbor. The *center* and *right* models were rotated 90° around the y axis and 90° around the x axis from the orientation shown on the *left* panel (c)

Table 3 SAXS structural parameters of hyperthermophilic esterase from *P. furiosus*

Parameters	Experimental (5 mg/mL)	DR model	Crystallographic model
R_g (Å)(Guinier)	21.4	–	–
R_g (Å)	19.72	–	16.45
D_{max} (Å)	55.0	–	52.27
SAXS resolution (Å)	20.02	20.02	–
Molecular weight (kDa)	30.7	–	–
χ^2	–	3.62	5.23

Table 4 Transesterification activity of *P. furiosus* esterase

Alcohol	Transesterification activity ($\times 10^{-2}$ $\mu\text{mol}/\text{min}\cdot\text{mg}$)
Methanol	0.21 ± 0.01
Ethanol	0.79 ± 0.09
2-propanol	0.78 ± 0.07
Isobutanol	2.69 ± 0.14

Pf_Est presented the same optimum temperature as the archaeon *Sulfolobus solfataricus* P1 [39], higher than *Bacillus licheniformis* S-86 (60 °C) and *Fervidobacterium nodosum* Rt17-B1 (75 °C) [40, 41]. On the other hand, the optimum temperature of Pf_Est is lower than that from *Thermotoga maritima* (95 °C), although it is important to highlight that in spite of the lower optimum temperature, Pf_Est is more stable than *T. maritima* esterase EstD [42].

In addition, thermal denaturation of Pf_Est was accompanied by the measurement of the change in ellipticity at 221 nm over the temperature range of 20–100 °C, showing that Pf_Est did not lose its secondary structure over this temperature range. These data reinforce the higher thermostability of Pf_Est when comparing to others previously described in the literature [36, 39, 42].

The kcat/km ratio of Pf_Est (3.02×10^{-2} (mmol/L)/s) using pNPP as substrate was similar to the ratio presented by lipase (189E r03Lip) from *Geobacillus* sp. (2.90×10^{-2} (mmol/L)/s) and higher than the bovine serum albumin at 70 °C (1.75×10^{-2} (mmol/L)/s) [43]. The kinetics parameters presented by Pf_Est indicates that it is an enzyme with great potential for use in biotechnological applications, especially in application at high temperatures.

Pf_Est showed a good stability toward solvents, showing high tolerance to immiscible solvents at the highest concentration (50 % v/v). This is an important characteristic once immiscible organic solvents are the preferred as reaction medium, once they provide greatest solubility of lipases target substrates [44]. On the other hand, miscible solvents are commonly used as substrates in esterification reactions mediated by lipases [45]. Thus, the stability in front of miscible solvents obtained by Pf_Est is also interesting for biotechnological applications.

The prediction of the secondary structure of Pf_Est performed using Jpre4 was in accordance with the canonical structure of esterases which consists of a highly twisted, 8–11-stranded beta-sheet in which most strands are parallel and this sheet is flanked on both sides by alpha-helices [46]. Guo et al. [47] observed the same pattern as it was observed in Pf_Est for a *Mycobacterium tuberculosis* esterase; however, esterases generally present a CD profile with predominance of alpha-helices [48–51], probably due to the presence of these structures in the external portion of the proteins. Moreover, SAXS analysis revealed a monomeric shape of Pf_Est in solution at its optimum temperature (80 °C). Collectively, CD and SAXS data reinforce the fact that the hyperthermophilic esterase from *P. furiosus* was successfully expressed by the mesophilic host (*E. coli*) preserving its correct fold and high stability.

The transesterifications values presented by the *P. furiosus* esterase for methanol, ethanol, and 2-propanol were lower than those obtained by [14] for wild and mutants lipases of *Geobacillus* sp. NTU03. The lowest transesterification value of Pf_Est was found when using methanol, the same pattern was observed lipases from *Geobacillus* sp. and *Candida antarctica* [13, 28]. On the other hand, the highest transesterification value of Pf_Est was found when using isobutanol as the acyl acceptor (more than three times higher than for the others alcohols). This is consistent with the general agreement that water-miscible polar solvents can strip off the water layer that forms around many proteins, which is essential for activity [52]. In contrast, nonpolar solvents may protect the microenvironment of enzymes, thereby preventing loss of the water layer.

The hydrolytic activity of *P. furiosus* esterase was determined and the enzyme was able to hydrolyze all lipids tested. The highest hydrolysis degree occurred using olive oil (6.2 U/mg), similar to Dharmstithi et al. [53] (4.8 U/mg) indicating good affinity for long-chain unsaturated fatty acids such as oleic acid, C18:1 *cis*-9 which is the predominant fatty acid in olive oil [54]. Soy oil (2.4 U/mg), waste cooking oil (1.8 U/mg), and corn oil (0.9 U/mg) were also hydrolyzed, which indicates Pf_Est hydrolysis ability against a broad spectrum of lipids, which can be interesting for detergent formulation increasing their effectiveness on different types of dirt [15].

Therefore, the extremely thermostable esterase described here presents potential to be used in a wide range of biotechnological applications such as synthesis and improvement of flavor esters and aroma in the food industry, modification of triglycerides in the oil industry, resolution of racemic mixtures for synthesis of pure chemicals in the pharmaceutical industry, as well as in the insecticides degradation and reduction of toxic compounds of plastic [8]. Thus, it refers to enzymes with great relevance and biotechnological potential, and therefore, the characterization is indispensable for effective and specific application.

In conclusion, this study describes the successful purification and characterization in terms of both functional and structural aspects of a hyper thermostable esterase from *Pyrococcus furiosus*, in addition to determination of the low-resolution structure of this enzyme by SAXS. Our findings provide biochemical and structural basis for further studies of esterases, indicating that Pf_Est may be suitable for applications in the chemical, food, and pharmaceutical industries.

Acknowledgments The authors would like to thank the Brazilian National Council for Scientific Research (CNPq) for financial support (310186/2014-5, 442333/2014-5, 313749/2014-0, and 140796/2013-4).

References

- Arpigny, J. L., & Jaeger, K. E. (1999). Bacterial lipolytic enzymes: classification and properties. *The Biochemical Journal*, *343*(Pt 1), 177–183.
- Anbu, P., Gopinath, S. C. B., Cihan, A. C., & Chaulagain, B. P. (2013). Microbial enzymes and their applications in industries and medicine. *BioMed Research International*, *2013*, 2–4.
- Jaeger, K. E., & Reetz, M. T. (1998). Microbial lipases form versatile tools for biotechnology. *Trends in Biotechnology*, *16*(9), 396–403.
- Jaeger, K. E., Schneidinger, B., Rosenau, F., Werner, M., Lang, D., Dijkstra, B. W., et al. (1997). Bacterial lipases for biotechnological applications. *Journal of Molecular Catalysis B Enzymatic*, *3*(1–4), 3–12.
- Ray, A. (2012). Application of lipase in industry. *Asian Journal of Pharmaceutical Technology*, *2*(2), 33–37.
- Kim, J., Deng, L., Hong, E., & Ryu, Y. (2015). Cloning and characterization of a novel thermostable esterase from *Bacillus gelatini* KACC 12197. *Protein Expression and Purification*, *116*, 90–97.
- Kawamoto, T., Sonomoto, K., & Tanaka, A. (1987). Esterification in organic solvents: selection of hydrolases and effects of reaction conditions. *Biocatalysis and Biotransformation*, *1*(2), 137–145.
- Panda, T., & Gowrishankar, B. S. (2005). Production and applications of esterases. *Applied Microbiology and Biotechnology*, *67*(2), 160–169.
- Cowan, D. (1992). Enzymes from thermophilic archaeobacteria: current and future applications in biotechnology. *Biochemical Society Symposia*, *58*, 149–169.
- Fiala, G., & Stetter, K. O. (1986). *Pyrococcus furiosus*; sp. nov. represents a novel genus of marine heterotrophic archaeobacteria growing optimally at 100 °C. *Archives of Microbiology*, *145*(1), 56–61.
- Ikeda, M., & Clark, D. S. (1998). Molecular cloning of extremely thermostable esterase gene from hyperthermophilic archaeon *Pyrococcus furiosus* in *Escherichia coli*. *Biotechnology and Bioengineering*, *57*(5), 624–629.
- Beaucage, S. L., & Iyer, R. P. (1992). Advances in the synthesis of oligonucleotides by the phosphoramidite approach. *Tetrahedron*, *48*(12), 2223–2311.
- Damásio, A. R. L., Braga, C. M. P., Brenelli, L. B., Citadini, A. P., Mandelli, F., Cota, J., et al. (2013). Biomass-to-bio-products application of feruloyl esterase from *Aspergillus clavatus*. *Applied Microbiology and Biotechnology*, *97*(15), 6759–6767.
- Shih, T.-W., & Pan, T.-M. (2011). Substitution of Asp189 residue alters the activity and thermostability of *Geobacillus* sp. NTU 03 lipase. *Biotechnology Letters*, *33*(9), 1841–1846.
- Sande, D., Souza, L. T. A., Oliveira, J. S., Santoro, M. M., Lacerda, I. C. A., Colen, G., et al. (2015). *Colletotrichum gloeosporioides* lipase: characterization and use in hydrolysis and esterifications. *African Journal of Microbiology Research*, *9*(19), 1322–1330.
- Mandelli, F., Franco Cairo, J. P. L., Citadini, A. P. S., Büchli, F., Alvarez, T. M., Oliveira, R. J., et al. (2013). The characterization of a thermostable and cambialistic superoxide dismutase from *Thermus filiformis*. *Letters in Applied Microbiology*, *57*(1), 40–46.
- Hammersley, A. P. (1997). FIT2D: an introduction and overview. *ESRF Internal Report ESRF97HA02*.
- Alvarez, T. M., Goldbeck, R., dos Santos, C. R., Paixão, D. A. A., Gonçalves, T. A., Franco Cairo, J. P. L., et al. (2013). Development and biotechnological application of a novel endoxylanase family GH10 identified from sugarcane soil metagenome. *PLoS One*, *8*(7), e70014.
- Svergun, D. I. (1992). Determination of the regularization parameter in indirect-transform methods using perceptual criteria. *Journal of Applied Crystallography*, *25*(pt 4), 495–503.
- Fischer, H., de Oliveira Neto, M., Napolitano, H. B., Polikarpov, I., & Craievich, A. F. (2009). Determination of the molecular weight of proteins in solution from a single small-angle X-ray scattering measurement on a relative scale. *Journal of Applied Crystallography*, *43*(1), 101–109.
- Kozin, M. B., & Svergun, D. I. (2001). Automated matching of high- and low-resolution structural models. *Journal of Applied Crystallography*, *34*(1), 33–41.
- Svergun, D., Barberato, C., & Koch, M. H. (1995). CRY SOL—a program to evaluate X-ray solution scattering of biological macromolecules from atomic coordinates. *Journal of Applied Crystallography*, *28*(6), 768–773.
- Rabbani, M., Bagherinejad, M. R., Sadeghi, H. M., Shariat, Z. S., Etemadifar, Z., Moazen, F., et al. (2013). Isolation and characterization of novel thermophilic lipase-secreting bacteria. *Brazilian Journal of Microbiology*, *44*(4), 1113–1119.
- Wang, L., Mavisakalyan, V., Tillier, E. R. M., Clark, G. W., Savchenko, A. V., Yakumin, A. F., et al. (2010). Mining bacterial genomes for novel arylesterase activity. *Microbial Biotechnology*, *3*(6), 677–690.
- Contesini, F. J., Calzado, F., Madeira, J. V., Rubio, M. V., Zubieta, M. P., de Melo, R. R., et al. (2016). *Aspergillus* lipases: Biotechnological and industrial application. In J. M. Mérillon & K. G. Ramawat (Eds.), *Reference series in phytochemistry: Fungal metabolites* (pp. 1–28). Cham, Switzerland: Springer International Publishing.

26. Bornscheuer, U. T. (2002). Microbial carboxyl esterases: classification, properties and application in biocatalysis. *FEMS Microbiology Reviews*, 26(1), 73–81.
27. Fullbrook, P. (1996). *Practical applied kinetics, industrial enzymology* (2nd ed.). New York: Stockholm Press.
28. Kelly, S., & Price, N. (2000). The use of circular dichroism in the investigation of protein structure and function. *Current Protein and Peptide Science*, 1(4), 349–384.
29. Greenfield, N. J. (2006). Using circular dichroism spectra to estimate protein secondary structure. *Nature Protocols*, 1(6), 2876–2890.
30. Guinier, A., & Fournet, G. (1955). Small angle scattering of X-rays. *Journal of Polymer Science*, 1, 268.
31. Schubot, F. D., Kataeva, I. A., Blum, D. L., Shah, A. K., Ljungdahl, L. G., Rose, J. P., et al. (2001). Structural basis for the substrate specificity of the feruloyl esterase domain of the celulosomal xylanase Z from *Clostridium thermocellum*. *Biochemistry*, 40(42), 12524–12532.
32. Carvalho, C. M. L., & Cabral, J. M. S. (2000). Reverse micelles as reaction media for lipases. *Biochimie*, 82, 1063–1085.
33. Chen, Q., Luan, Z.-J., Cheng, X., & Xu, J.-H. (2015). Molecular dynamics investigation of the substrate binding mechanism in carboxylesterase. *Biochemistry*, 54(9), 1841–1848.
34. Rattray, F. P., & Fox, P. F. (1997). Purification and characterization of an intracellular aminopeptidase from *Brevibacterium linens* ATCC 9174. *Lait*.
35. Fuciños, P., Atanes, E., López-López, O., Esperanza Cerdán, M., Isabel González-Siso, M., Pastrana, L., et al. (2011). Production and characterization of two N-terminal truncated esterases from *Thermus thermophilus* HB27 in a mesophilic yeast: effect of N-terminus in thermal activity and stability. *Protein Expression and Purification*, 78(2), 120–130.
36. Ayna, Ç., Kolcuoğlu, Y., Öz, F., Colak, A., & Ertunga, N. S. (2013). Purification and characterization of a pH and heat stable esterase from *Geobacillus* sp. TF17. *TurkJBiochem*, 4685, 329–336.
37. Almeida, R., Alqueres, S., Larentis, A., Rossle, S., Cardoso, A., Almeida, W., et al. (2006). Cloning, expression, partial characterization and structural modeling of a novel esterase from *Pyrococcus furiosus*. *Enzyme and Microbial Technology*, 39(5), 1128–1136.
38. Chandrayan, S. K., Dhaunta, N., & Guptasarma, P. (2008). Expression, purification, refolding and characterization of a putative lysophospholipase from *Pyrococcus furiosus*: retention of structure and lipase/esterase activity in the presence of water-miscible organic solvents at high temperatures. *Protein Expression and Purification*, 59(2), 327–333.
39. Nam, J.-K., Park, Y.-J., & Lee, H.-B. (2013). Cloning, expression, purification, and characterization of a thermostable esterase from the archaeon *Sulfolobus solfataricus* P1. *Journal of Molecular Catalysis B: Enzymatic*, 94, 95–103.
40. Torres, S., Baigorri, M. D., Swathy, S. L., Pandey, A., & Castro, G. R. (2009). Enzymatic synthesis of banana flavour (isoamyl acetate) by *Bacillus licheniformis* S-86 esterase. *Food Research International*, 42(4), 454–460.
41. Yu, S., Zheng, B., Zhao, X., & Feng, Y. (2010). Gene cloning and characterization of a novel thermophilic esterase from *Fervidobacterium nodosum* Rt17-B1. *Acta Biochimica et Biophysica Sinica*, 42(4), 288–295.
42. Levisson, M., van der Oost, J., & Kengen, S. W. M. (2007). Characterization and structural modeling of a new type of thermostable esterase from *Thermotoga maritima*. *The FEBS Journal*, 274(11), 2832–2842.
43. Córdova, J., Ryan, J. D., Boonyaratankornkit, B. B., & Clark, D. S. (2008). Esterase activity of bovine serum albumin up to 160 °C: a new benchmark for biocatalysis. *Enzyme and Microbial Technology*, 42(3), 278–283.
44. Tamalampudi, S., Hama, S., Tanino, T., Talukder, M. R., Kondo, A., & Fukuda, H. (2007). Immobilized recombinant *Aspergillus oryzae* expressing heterologous lipase: an efficient whole-cell biocatalyst for enantioselective transesterification in non-aqueous medium. *Journal of Molecular Catalysis B: Enzymatic*, 48(1–2), 33–37.
45. Mustranta, A., Forssell, P., & Poutanen, K. (1993). Applications of immobilized lipases to transesterification and esterification reactions in nonaqueous systems. *Enzyme and Microbial Technology*, 15(2), 133–139.
46. Marchot, P., & Chatonnet, A. (2012). Enzymatic activity and protein interactions in alpha/beta hydrolase fold proteins: moonlighting versus promiscuity. *Protein and Peptide Letters*, 19(2), 132–143.
47. Guo, J., Zheng, X., Xu, L., Liu, Z., Xu, K., Li, S., et al. (2010). Characterization of a novel esterase Rv0045c from *Mycobacterium tuberculosis*. *PLoS One*, 5(10), e13143.
48. Rhee, J. K., Kim, D. Y., Ahn, D. G., Yun, J. H., Jang, S. H., Shin, H. C., et al. (2006). Analysis of the thermostability determinants of hyperthermophilic esterase EstE1 based on its predicted three-dimensional structure. *Applied and Environmental Microbiology*, 72(4), 3021–3025.
49. Dang, G., Chen, L., Li, Z., Deng, X., Cui, Y., Cao, J., et al. (2015). Expression, purification and characterisation of secreted esterase Rv2525c from *Mycobacterium tuberculosis*. *Applied Biochemistry and Biotechnology*, 176(1), 1–12.
50. Benavente, R., Esteban-Torres, M., Acebrón, I., De Las Rivas, B., Muñoz, R., Álvarez, Y., et al. (2013). Structure, biochemical characterization and analysis of the pleomorphism of carboxylesterase Cest-2923 from *Lactobacillus plantarum* WCFS1. *FEBS Journal*, 280(24), 6658–6671.
51. Li, P. Y., Ji, P., Li, C. Y., Zhang, Y., Wang, G. L., Zhang, X. Y., et al. (2014). Structural basis for dimerization and catalysis of a novel esterase from the GTSAG motif subfamily of the bacterial hormone-sensitive lipase family. *Journal of Biological Chemistry*, 289(27), 19031–19041.
52. Gupta, M. N. (1992). Enzyme function in organic solvents. *European Journal of Biochemistry/FEBS*, 203(1992), 25–32.
53. Dharmsthiti, S., & Luchai, S. (1999). Production, purification and characterization of thermophilic lipase from *Bacillus* sp. THL027. *FEMS Microbiology Letters*, 179(2), 241–246.
54. Pastore, G. M., Costa, V. D., & Koblitz, M. G. (2003). Production, partial purification and biochemical characterization of a novel *Rhizopus* sp. strain lipase. *Food Science and Technology (Campinas)*, 23(2), 135–140.